Journal of Inorganic and Organometallic Polymers and Materials (2023) 33:2346–2353
https://doi.org/10.1007/s10904-023-02663-3

RESEARCH

Impact of Hydrothermal Treatment on the Porous Structure and Adsorption Properties of Spherically Granulated Zirconium Silicate

Mykola V. Kravchenko[1] · Olena A. Diyuk[1,2] · Igor Z. Zhuravlev[1] · Svitlana I. Meleshevych[1] · Iryna V. Romanova[1]

Received: 3 February 2023 / Accepted: 16 April 2023 / Published online: 8 May 2023

Abstract
In the present study the spherically granulated micro- and mesoporous zirconium silicates were prepared and thermally treated in the wide region of temperatures 110–700 °C. Physico-chemical properties of materials obtained were investigated by powder X-ray diffraction, low-temperature nitrogen adsorption/desorption method and scanning electron microscopic studies. It was found that calcination leads to significant decreasing the surface area and total pore volumes of zirconium silicates. After hydrothermal treatment of spherically granulated material previously dried at room temperature the positive changes of porous structure with significant increasing the total surface area and volume of mesopores it was fixed. Adsorption properties of as-prepared samples and obtained after thermal and hydrothermal treatments in the process of removing Cu^{2+}, Ni^{2+} and Co^{2+} cations from water solution were examined. It was determined that zirconium silicate hydrothermally treated at 300 °C during 5 h hours has the biggest surface area and shows the lowest decreasing adsorption capacity among sorbents calcined toward cobalt and nickel ions and could be used as perspective material for effective removing the d-metal ions at high temperatures.

Keywords Spherically granulated zirconium silicates · Effect of hydrothermal treatment · Morphology · Adsorption at high temperatures · Heavy metals removing

1 Introduction

Interest of researchers to design a new low-cost method for obtaining the natural friendly adsorbents deals with the large number of inorganic toxicants (first of all, radionuclides and heavy metals) in water as result by human activity [1–3]. Several treatment and separation techniques have been used to minimize the concentration level of pollutants content including the ion-exchange, coagulation, lime precipitation, solvent extraction, electrolytic processes and other approaches. Adsorption is regarded as one of the most powerful treatment methods because of its low costs, convenience, and wide adaptability [4–7]. Different adsorbents are highly effective for toxicants removing such as materials based on the natural clay [8–10], carbon [11], a number of inorganic synthetic materials based on the individual and mixed metal oxides [12–16], titanates [17], phosphates [18], silicates [19], etc.

Zirconium silicate is introduced in many applications. It has been used as a filler material in fire retardant coatings, as it is characterized by thermal stability and chemical inertness at high temperature [4, 20]. These materials have attracted the attention of scientists in the field of medicine and radiochemistry due to its ability to selectively adsorb a lot of ions such as ammonium, potassium, cesium, strontium, and a number of actinoids. For example, well known sorbents have been obtained from zirconium alkoxy compounds using hydrothermal synthesis in crystalline form by A. Clierfield and coauthors [21–24] and their ion exchange behavior towards alkali metal ions has been carefully studied. Currently, zirconium silicates in the amorphous or poorly crystalline forms with developed porous structure are more successfully used as sorbents and catalysts [25–30].

✉ Iryna V. Romanova
irom@bigmir.net

[1] Institute for Sorption and Problems of Endoecology, NAS of Ukraine, 13 General Naumov Str., Kiev 03164, Ukraine

[2] M.G. Kholodny Institute of Botany, NAS of Ukraine, 2 Tereshchenkivska Str., Kiev 01004, Ukraine

Among methods often used for preparing the same materials the most popular are precipitation and sol–gel technology, a lot of works have been devoted the hydrothermal [31, 32] and microwave [33] treatments of precursor that improves the physico-chemical properties of materials obtained, first of all, the porous structure of materials. Synthesis of highly porous spherically granulated zirconium silicate from aqueous solutions of cheap, available salts has been described early [34]. One step of method includes the addition to aqueous solution of zirconium chloride an excess of potassium carbonate that leads to the formation of metastable anionic carbonate complexes (precursor). Treatment of such complexes with an aqueous solution of sodium metasilicate causes the gel formation. An additional application of droplet coagulation technology [35–37] ensured the production of spherically granulated ZrO_2–SiO_2 hydrogel.

In this paper, our primary aim is to investigate the properties of as-prepared and thermally treated spherically granulated zirconium silicate. Investigation the morphology of initial and treated materials is carried out by XRD analysis, scanning electron microscope (SEM) studies, low temperature adsorption/desorption technology. Adsorption properties of samples have been examined in the process of removing the d-metal ions (Cu^{2+}, Co^{2+} and Ni^{2+}) from water solution. Experimental adsorption data obtained are fitted into the Langmuir model. Data obtained has showed the possibility to use materials after hydrothermal treatment for purification water from cobalt and nickel ions at high temperatures (for example in radioactive waste treatment [38, 39]) with the storage of the initial adsorption capacity.

2 Experimental Details

All chemicals used ($ZrOCl_2 \cdot 8H_2O$, $K_2CO_3 \cdot 2H_2O$, $Cu(NO_3)_2 \cdot 3H_2O$, $Co(NO_3)_2 \cdot 6H_2O$ and $Ni(NO_3)_2 \cdot 6H_2O$) were of analytical grade and used without previous purification. The aqueous sodium metasilicate solution of SiO_2/Na_2O molar ratio = 3.14, Na_2O—9.3%, SiO_2—28%, density—1.42 g/L was produced by Ukrainian enterprise (PJSC "Zaporizhskloflus") and analyzed by acid-basic titration method. Initial and equilibrium concentration of metals in solution for adsorption experiment was measured by atomic absorption spectrometer.

X-ray diffraction (XRD) patterns were obtained on a DRON-4-07 diffractometer (LOMO, Russia) using CuKα radiation (λ = 0.15418 nm) in the 2θ angle range of 10–60° with a 0.02 step. To qualitatively determine the phase composition of samples JCPDS-ICDD data base was used. Relative intensities and widths of lines were calculated by means of a PFM software (Origin Module Pack File). Average crystallite size was calculated according to the line width method based on the Debye–Scherrer equation [40].

In the term of understanding the morphology of zirconium silicate obtained scanning electron microscopes (SEM) investigation was done with a JEM 6060 and JSM 7001F with an microanalyzer system (JEOL, Japan).

Specific surface areas and pore size distributions for the synthesized samples and after thermal treatment were calculated from nitrogen adsorption/desorption curves (NOVA 2200e, Quantachrome, USA) using the Nova Win 2.0 software. The total surface area of the materials S_{total} was calculated by the Brunauer–Emmet–Teller method (BET). The total pore volume (V_{total}) was calculated from the volume of nitrogen adsorbed converted to liquid at a pressure close to $P/P_0 = 1$. To acquire the volume of mesopores (V_{meso}), Barrett–Joyner–Halenda (BJH) method was used. The micropore volume (V_{micro}) was calculated by subtracting the value of V_{meso} from V_{total}. The average pore radii (R_{pore}) was determined from the total pore volume (V_{total}) of the materials and its specific surface area (S_{total}) by equation $R_{pore} = 2V_{total}/S_{total}$. Pore radii distributions were obtained from isotherms in terms of the density functional theory (DFT).

Sorption properties of as-prepared and treated samples were studied after 4 h shaking and one day of static contact (solid:liquid = 1:500). Concentrations of Cu^{2+}, Co^{2+} and Ni^{2+} in initial and equilibrium solutions of nitrates were measured using Shimadzu AA 6300 (Shimadzu, Japan) atomic adsorption analyzer. All the adsorption measurements were repeated twice to assure the reproducibility of the obtained results.

Adsoption capacity (q_e, mmol/g) was calculated by the well-known equation:

$$q_e = (C_0 - C_e)V/m, \tag{1}$$

where C_0 and C_e are the initial and equilibrium metal concentration in solution, respectively, mmol/L; V is the aliquot volume (L); and m is the mass of the adsorbent (g).

Experimental data were fitted into the Langmuir model, that is commonly used to describe liquid–solid systems [41] by the following equations:

$$q_e = Q_0 K_L C_e/(1 + K_L C_e), \tag{2}$$

where q_e is the adsorption capacity (mmol/g); C_e is the equilibrium concentration of the adsorbate (mmol/L); Q_0 is the maximum adsorption capacity of the adsorbent (mmol/g); and K_L is the Langmuir sorption equilibrium constant (L/mmol). To evaluate the correlation between the experimental data and theoretical models, the coefficient of determination (R^2) was calculated.

3 Results and Discussion

3.1 Morphology of Spherically Granulated Zirconium Silicates

Method used for material producing in this work involves the mixing of $ZrOCl_2$ solution (2 M) and the solution of K_2CO_3 (5 M) with the vigorous stirring of mixture that has finished by formation of a zirconium carbonate complex. Solution of complex has been mixed in desired proportion with a sodium metasilicate solution (necessary to obtain a Zr/Si ratio of 0.6 [34]), then mixture has been fed at a rate of 100 mL/min into a flow reactor in which the solutions are mixed to form a zirconium oxyhydrate and silicic acid. Sol obtained is directed into a column filled with two layers of liquids: the top layer is undecane, and the bottom is running tap water. During the passage of the undecane layer (1.0–1.5 m), the sol stream is broken into separate drops, which in 3–5 s turned into durable spherical granules of Zr–Si hydrogel. They are transferred with water and first fell on a sieve, and then into a container, where they have been washed by distilled water from alkalis, salts and traces of undecane, washed with water until neutral pH. Granules obtained have been dried by two steps—at room temperature (25 °C) and then at 110 °C in the oven for physically adsorbed water removing. Hydrothermal treatment of granules before drying is carried out in stainless steel autoclave.

SEM micrographs for spherically granulated zirconium silicate (dried at 110 °C) with various times magnification are presented in Fig. 1a–d. It is seen that granules are well spherically defined and have a size from 200 up to 500 μm (a), sometimes it has been fixed granules an about 900 μm (b). After the targeted cleavage of the largest granule, it is turned out its internal structure contains layers and voids (b). At great magnifications it is noticeable, the surface of the granules is porous, rather homogeneous in structure (c, d), consists on unisize particles with the mesopores. The elemental composition of the sample done by microanalyzer has been showed the amount of zirconium dioxide included in the structure of the obtained gel is less than that taken for the synthesis and the real Zr/Si ratio in it is ~ 0.45.

The influence of the calcination temperature on the structural parameters has been studied using the XRD technique. At first, zirconium silicate samples have been thermally treated (TT) at various temperatures (300, 500, 700 and 1000 °C) and X-ray diffraction patterns as-prepared and calcined are presented in Fig. 2. The absence of reflections up to 700 °C indicates that these materials are amorphous. As has been published earlier [42] after thermal treatment of zirconia–silica mixed oxides taken with Zr/Si ratio ~ 0.45 in region of temperatures 300–1200 °C two crystalline forms—zircon $ZrSiO_4$ and monoclinic zirconia ZrO_2 can be found. Data presented in Fig. 2 shows that diffraction pattern of spherically granulated zirconium silicate after treatment at 1000 °C does not contain the peaks characteristic of these crystalline phases. The reflection peaks that

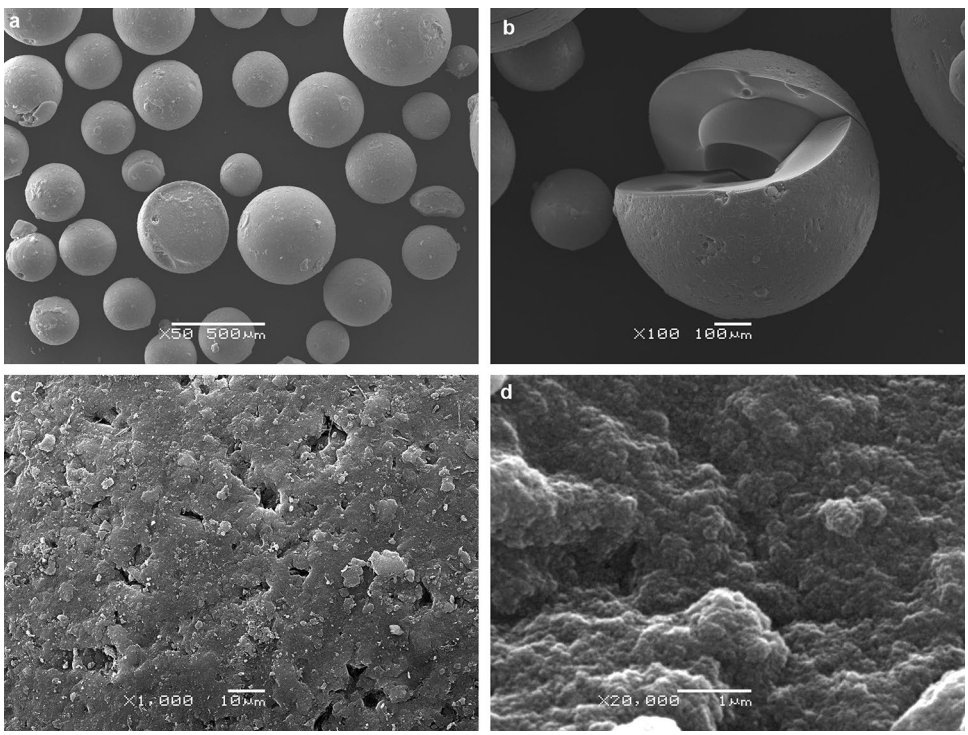

Fig. 1 SEM micrographs for spherically granulated zirconium silicate dried at 110 °C with ×30 magnification (**a**), ×100 (**b**), ×1000 (**c**) and ×20,000 magnification (**d**)

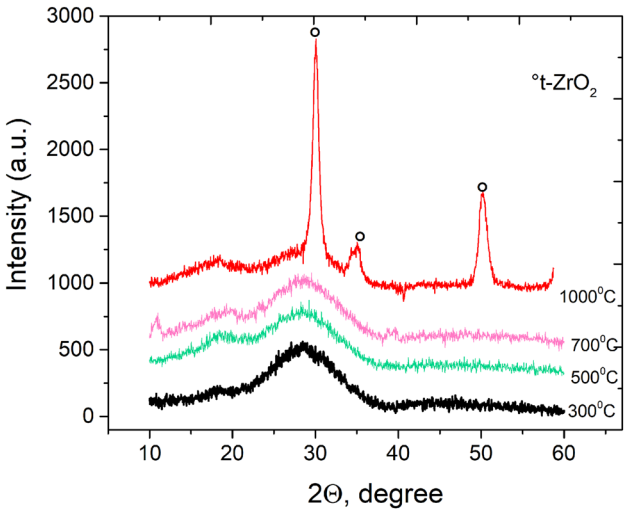

Fig. 2 X-ray diffraction data for spherically granulated zirconium silicate thermally treated at 300, 500, 700 and 1000 °C

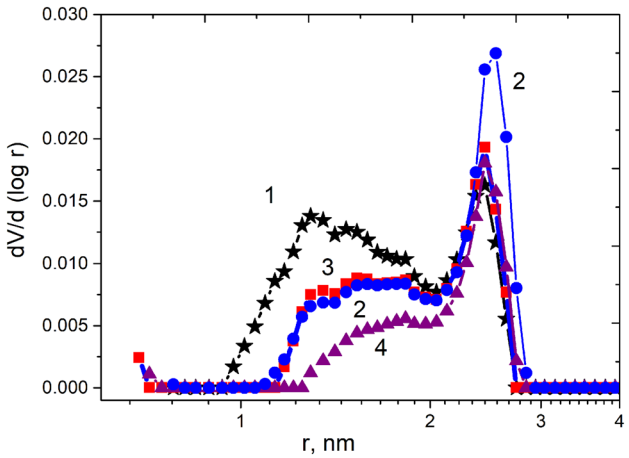

Fig. 3 Pore size distribution obtained in term of DFT method for initial spherically granulated zirconium silicate dried at room temperature (1) and 110 °C (2), samples thermally treated at 300–500 (3) and 700 °C (4)

occurred at 2θ = 30.4°, 35.3°, 50.5° have been ascribed to tetragonal phase of ZrO_2 (ICDD No. 01-079-1764) that usually is formed at higher temperature. This phase could be obtained at temperatures below 800 °C only using special approaches, for example method Pechini that guaranties the formation of various crystal phases at lower temperatures then obtained by solid state reaction [43, 44]. The size of particles determined using broadening of the most intensive reflex is 7.5 nm.

Porous structure of initial and thermally treated materials has been studied by method of low temperature adsorption/desorption of nitrogen, these data are presented in the Table 1 and in Fig. 3. It is seen that treatment the sample at 110 °C (after room temperature drying) has changed the main porous characteristics of material. It has been fixed decreasing the total surface area, total pore volume does not change while the volume of mesopores increases an about twice. Further increasing the temperature of treatment leads to significant decreasing the surface area, total pore volume, including the micro- and of mesopore volumes (Table 1). It has not been fixed the strong correlation between increasing the temperature of treatment and average pore radii of samples.

More detailed analysis of pore size distribution has been provided by DFT method. Data presented in Fig. 3 show the significant decreasing the pores radii ~ 1.4–1.6 nm with increasing of temperature, volume of pores radii 2.5 nm has significant decreased from 110 up to 300 °C whereas the further increasing of temperature do not cause the changes.

Table 1 Porosity data for spherically granulated zirconium silicate dried at temperature 25 and 110 °C, thermally treated at 300, 500 and 700 °C

Thermal treatment, °C	25	110	300	500	700
BET surface area, S_{total} (m^2/g)	363	267	236	220	144
Total pore volume, V_{total} (cm^3/g)	0.23	0.21	0.21	0.16	0.14
Mesopore volume, V_{meso} (cm^3/g)	0.08	0.19	0.08	0.08	0.08
Micropore volume, V_{micro} (cm^3/g)	0.15	0.02	0.13	0.08	0.06
Average pore radius, R_{pore} (nm)	1.3	1.6	1.8	1.5	1.9

3.2 Hydrothermal Treatment of Spherically Granulated Zirconium Silicates

It is known that hydrothermal treatment of precursors promotes the formation of final materials with well-developed hierarchical pore structure first of all with high specific surface area [39, 45–47]. Therefore, the next step of investigation has been devoted to search the optimal condition for hydrothermal treatment of spherically granulated zirconium silicate aimed to obtain the material with the best porous characteristics. We have investigated the properties of materials after thermal and hydrothermal treatment for determining the possibilities of application them as sorbents for evaluation of corrosion products in primary coolant circuit of NPP [38] (~ 300 °C). Temperature 180 °C has been chosen as average between room temperature drying and 300 °C. Pore size distributions (DFT method) for initial spherically granulated zirconium silicate dried at room temperature (25 °C) and samples hydrothermally treated during various time and the main characteristic of porous structure of as-prepared and samples obtained after hydrothermal treatment are presented in Fig. 4 and Table 2.

As follows from presented pore size distribution hydrothermal treatment significantly changes the porous structure

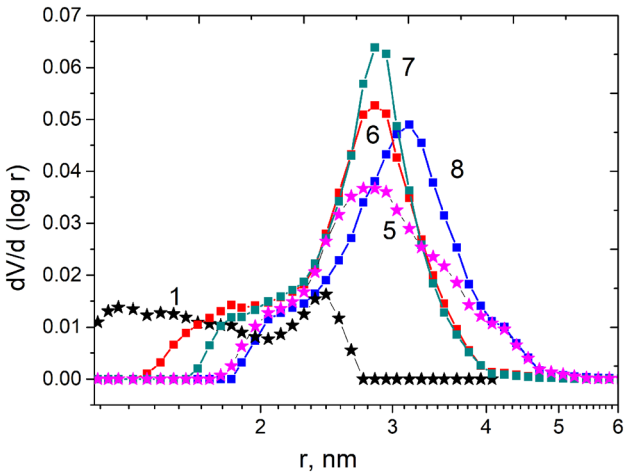

Fig. 4 Pore size distribution obtained in term of DFT method for initial spherically granulated zirconium silicate dried at room temperature 25 °C (1) and samples hydrothermally treated at temperatures 180 °C during 5 h (5), 300 °C during 5 (6), 12 (7) and 72 h (8)

of samples (Fig. 4). First of all, it has been fixed the formation of pores radii 2.3–5 nm for all samples and the disappearance of micropores after treatment at 300 °C. The biggest amount of new formed mesopores has the sample treated at 300 °C during 12 h. As follows from data received by porosity studies (Table 2) temperature and time of hydrothermal treatment significantly impact on the main characteristics of materials. The greatest surface area shows the sample treated at 300 °C during 5 h whereas after treatment at 180 °C surface area increasing is negligible. Change the time of treatment from 5 up to 12 h leads to decrease the surface area (Table 2) and increase the volume of pores radii ~ 2.8 nm. Previous drying of samples at 110 and 300 °C does not positively impacts on these characteristics.

3.3 Adsorption Capacity of As-Prepared and Calcined Spherically Granulated Zirconium Silicates Towards Heavy Metal Ions

Adsorption properties of initial materials and obtained after thermal and hydrothermal treatment have been examined in the process of removing the copper, cobalt and nickel ions from water solution at pH = 5–6. To evaluate the adsorption capacity at different initial concentration, 0.025 g of samples has been added to 25 mL (solid:liquid = 1:100) of metals aqueous solution with concentration of 0.1–5 mmol/L. Resulting mixtures are shacked for 4 h, and left for 1 day at 25 °C, after which the sorbents are removed by means of filtration and the metals content in filtrates are determined, data are presented in Fig. 5 and in Table 3.

It is known that Langmuir model assumes monolayer adsorption (the adsorbed layer is one molecule in thickness), with adsorption can only occur at a fixed number of definite localized sites, that are identical and equivalent, with no lateral interaction and steric hindrance between the adsorbed molecules [41]. High dispersion coefficients (Table 3) seems that Langmuir model fits well for d-metal sorption by this adsorbent, so calculated maximum of adsorption (Q_0) has been used in discussion of adsorption properties.

Obviously, that as-prepared spherically granulated zirconium silicate exhibits the high adsorption capacity towards ions investigated (Q_0 = 0.82–1.22 mmol/g, Table 3). For copper ions capacity of materials after thermal treatment decreases more than twice from 1.22 up to 0.40 mmol/g. It is found for samples after hydrothermal treatment the adsorption capacity is lower than for samples after thermal treatment (~ 0.24–0.30 mmol/g). Another way to change the adsorption properties after treatment has been fixed for cobalt and nickel ions removing. The decreasing of capacity in these cases is not so significant that can be explained by great increasing the total surface area due to form mesopores. For example, adsorption of cobalt on the sorbent obtained by hydrothermal treatment of zirconium silicate at 180 °C during 12 h is 0.74 mmol/g while on the

Table 2 Porosity data for spherically granulated zirconium silicate hydrothermally treated at temperatures 180 and 300 °C

Pretreatment temperature, °C	Hydrothermal treatment		BET surface area, S_{total} (m^2/g)	Total pore volume, V_{total} (cm^3/g)	Average pore radius, R_{pore} (nm)
	Temperature	Time			
25	–	–	363	0.23	1.3
25	180	12	388	0.42	2.2
25	300	5	517	0.60	2.3
25	300	12	494	0.60	2.4
25	300	72	460	0.65	2.8
110	180	12	211	0.26	2.5
300	180	12	183	0.21	2.3

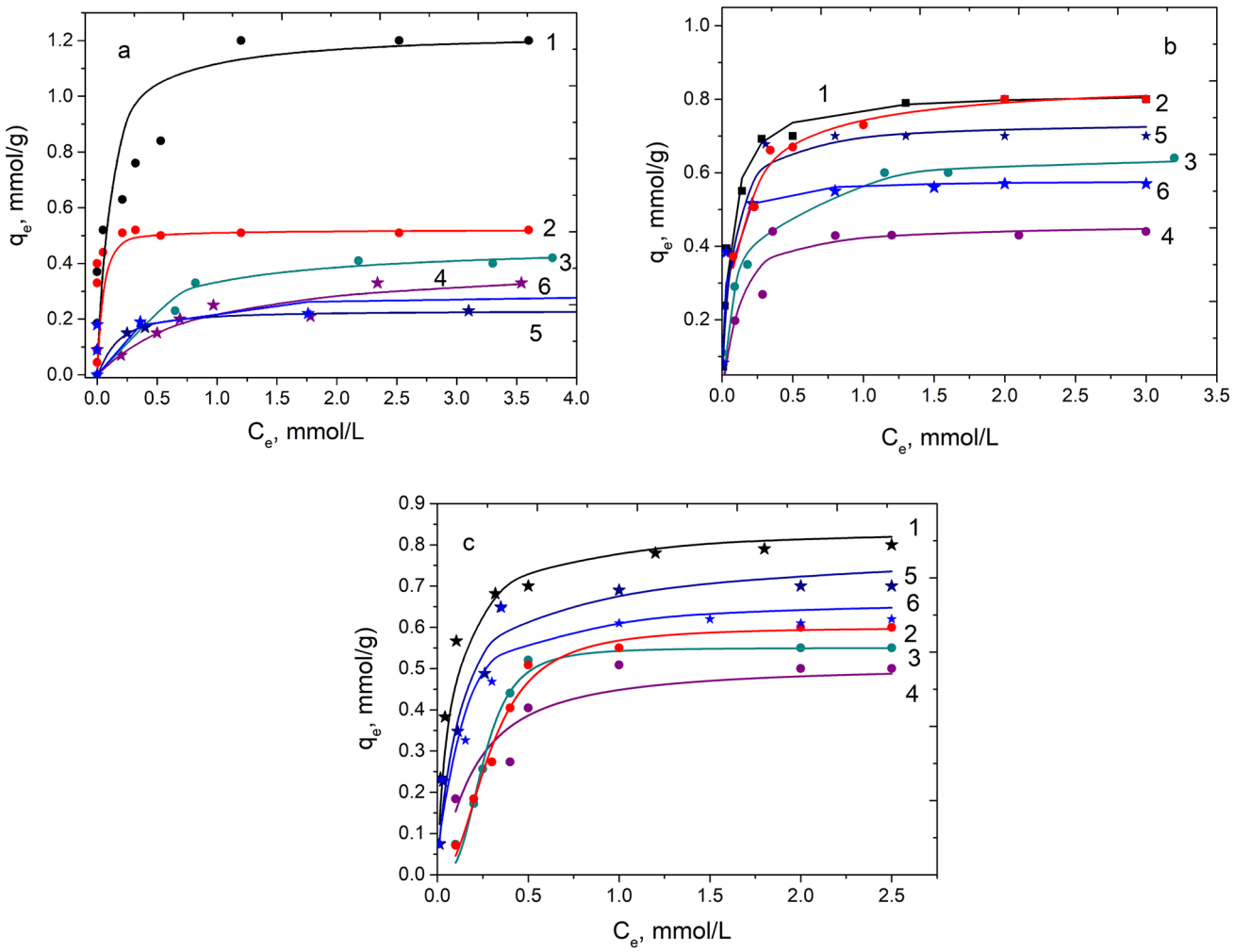

Fig. 5 Adsorption isotherms for copper (**a**), cobalt (**b**) and nickel (**c**) for samples spherically granulated zirconium silicate dried at room temperature (1), thermal treated at 300 (2), 500 (3), and 700 °C (4), hydrothermal treated at 180 °C for 12 h (5) and 300 °C for 5 h (6)

Table 3 Langmuir parameters of copper, cobalt and nickel adsorption for spherically granulated zirconium silicate thermally (TT) and hydrothermally treated (HTT) at various temperatures

Treatment, °C	TT, 25	TT, 300	TT, 500	TT, 700	HTT, 180	HTT, 300
Adsorption						
Cu^{2+}						
Q_0 (mmol/g)	1.22	0.52	0.46	0.40	0.24	0.30
K_L (L/mmol)	12.9	58.6	2.71	1.22	4.96	4.12
R^2	0.92	0.92	0.99	0.99	0.96	0.97
Co^{2+}						
Q_0 (mmol/g)	0.84	0.82	0.65	0.46	0.74	0.58
K_L (L/mmol)	8.75	17.7	10.3	12.3	18.3	37.5
R^2	0.99	0.98	0.98	0.98	0.99	0.99
Ni^{2+}						
Q_0 (mmol/g)	0.82	0.70	0.69	0.55	0.76	0.67
K_L (L/mmol)	14.3	1.88	1.90	4.43	10.1	11.8
R^2	0.99	0.98	0.98	0.99	0.98	0.96

initial—0.84. For process removing of nickel these values are identical—0.76 and 0.82, respectively.

It is interesting to compare the sorption properties of spherically granulated zirconium silicate with similar materials synthesized early. It is found that amorphous powders based on the zirconium silicate have the greatest capacity towards ions investigated [25, 26] while the capacity of spherically granulated titanium and zirconium phosphate towards d-metals obtained by same method equals to sample presented [35–37].

4 Conclusions

In summary, the spherically granulated zirconium silicate is synthesized through the stage of zirconium carbonate complex formation and application of droplet coagulation technology. It is determined by scanning electron microscopes studies that granules are well spherically defined and have a size from 200 up to 500 μm. The elemental composition of the sample done by microanalyzer has been showed the Zr/Si ratio in it is ~ 0.45 (0.65 taken for synthesis). XRD investigation of zirconium silicate shows that materials are amorphous after thermal treatment up to 1000 °C while further increasing the temperature leads to form the tetragonal phase of ZrO_2. After thermal treatment it has fixed decreasing the total surface area when the hydrothermal treatment causes the significant increasing the surface area and total pore volumes due to formation the pores radii 2.3–5 nm. Adsorption capacity towards copper ions linearly decreases after thermal and hydrothermal treatment more than five times from 1.22 up to 0.24 mmol/g. Despite of disappearance of micropores it has not been fixed the significant decreasing of capacity towards nickel and cobalt ions for hydrothermally treated materials due to great increasing the total surface area. Overviewing the results of studies one can rich the conclusions that spherically granulated zirconium silicate after hydrothermal treatment improves the porous structure and could be used as the sorbent for removing of cobalt and nickel ions at high temperatures with the storage of initial capacity.

Acknowledgements Financial support for this study has been provided by National Academy of Sciences of Ukraine within the framework of the target research program "Synthesis and physicochemical studies of composite materials for environmental purposes based on natural and synthetic silicates", 2022-2024. The authors thank O. I. V'yunov for his help in carrying out XRD measurements and M. M. Tsyba for supporting the porous investigations the materials.

Author contributions All authors contributed to the study conception and design. Material preparation and morphology investigation were performed by MVK and IZZ, adsorption data collection and analysis were performed by SIM. OAD was carrying out all SEM measurements.The first draft of the manuscript was written by IR and all authors commented on previous versions of the manuscript. All authors read and approved the final manuscript.

Funding The authors have not disclosed any funding.

Declarations

Competing interests The authors declare no competing interests.

References

1. K.A. Kydralieva, G.I. Dzhardimalieva, A.A. Yurishcheva, S.J. Jorobekova, J. Inorg. Organomet. Polym. **26**, 1212 (2016). https://doi.org/10.1007/s10904-016-0436-1
2. R. Kumar, M.A. Laskar, I.F. Hewaidy, M.A. Barakat, Earth. Syst. Environ. **3**, 83 (2019). https://doi.org/10.1007/s41748-018-0085-3
3. I. Ihsanullah, M. Sajid, S. Khan, M. Bilal, Sep. Purif. Technol. **291**, 120923 (2022). https://doi.org/10.1016/j.seppur.2022.120923
4. M.E. Mahmoud, G.M. Nabil, S.M.E. Mahmoud, J. Environ. Chem. Eng. **3**(2), 1320 (2015). https://doi.org/10.1016/j.jece.2014.11.027
5. B. Zhang, Y. Wu, Y. Fan, J. Inorg. Organomet. Polym. **29**, 290 (2019). https://doi.org/10.1007/s10904-018-0987-4
6. J. Qu, X. Tian, Zh. Jiang, B. Cao, M.S. Akindolie, Q. Hu, Ch. Fenga, Y. Fenga, X. Meng, Y. Zhang, J. Hazard. Mater. **387**, 121718 (2020). https://doi.org/10.1016/j.jhazmat.2019.121718
7. P. Shende, N.P. Devlekar, Curr. Nanosci. **17**(6), 819 (2021). https://doi.org/10.2174/1573413716999201209105819
8. S. Gupta, S. Sireesha, I. Sreedhar, Ch.M. Patel, K.L. Anitha, J. Water Process Eng. **38**, 101561 (2020). https://doi.org/10.1016/j.jwpe.2020.101561
9. C. Hood, E. Pensini, Water Air Soil Pollut. **233**, 137 (2022). https://doi.org/10.1007/s11270-022-05609-6
10. R.S. Hassan, M.R. Abass, M.A. Eid, E.A. Abdel-Galil, Appl. Radiat. **178**, 109985 (2021). https://doi.org/10.1016/j.apradiso.2021.109985
11. M. Nasrollahzadeh, M. Sajjadi, S. Iravani, R.S. Varmac, Chemosphere **263**, 128005 (2021). https://doi.org/10.1016/j.chemosphere.2020.128005
12. D.V. Tarnovsky, M.M. Tsyba, L.S. Kuznetsova, T.A. Khodakovska, I.V. Romanova, J. Chem. Technol. **29**(2), 192 (2021). https://doi.org/10.15421/jchemtech.v29i2.232199
13. D. Bhatt, N. Gururani, A. Srivastava, PCh. Srivastav, Environ. Earth. Sci. **80**, 273 (2021). https://doi.org/10.1007/s12665-021-09566-x
14. S. Safari, B.G. Lottermoser, D.S. Alessi, Appl. Mater. Today **19**, 100638 (2020). https://doi.org/10.1016/j.apmt.2020.100638
15. I.Z. Zhuravlev, M.F. Kovtun, A.V. Botsman, Sep. Sci. Technol. (2021). https://doi.org/10.1080/01496395.2021.1934024
16. P. Vassileva, P. Tzvetkova, L. Lakov, O. Peshev, J. Porous Mater. **15**, 593 (2008). https://doi.org/10.1007/s10934-007-9138-y
17. H. Li, Y. Huang, J. Liu, H. Duan, Chemosphere **282**, 131046 (2021). https://doi.org/10.1016/j.chemosphere.2021.131046
18. M. Maslova, N. Mudruk, A. Ivanets, I. Shashkova, N. Kitikova, Environ. Sci. Pollut. Res. **27**, 3933 (2020). https://doi.org/10.1007/s11356-019-06949-3
19. D.V. Tarnovsky, I.K. Chepurna, S.I. Meleshevych, V.I. Davydov, I.V. Romanova, Res. Chem. Intermed. **48**, 2253 (2022). https://doi.org/10.1007/s11164-022-04691-z
20. Zh. Dinga, M. Ridley, J. Deijkers, N. Liu, Sh. Bin Hoque, J. Gaskins, M. Zebarjadi, P. Hopkins, H.Wadley, E. Opila, K. Esfarjani, Materialia **12**, 100793 (2020). https://doi.org/10.1016/j.mtla.2020.100793.
21. A.I. Bortun, L.N. Bortun, A. Clearfield, Chem. Mater. **9**, 1854 (1997). https://doi.org/10.1021/cm9701419

22. A. Clearfield, A.I. Bortun, L.N. Bortun, D.M. Poojary, S.A. Khainakov, J. Mol. Struct. **470**, 207 (1998). https://doi.org/10.1016/S0022-2860(98)00482-7
23. Ch.S. Fewox, Sh.R. Kirumakki, A. Clearfield, Chem. Mater. **19**, 384 (2007). https://doi.org/10.1021/cm061835x
24. Ch.S. Fewox, A. Clearfield, J. Phys. Chem. A **112**, 2589 (2008). https://doi.org/10.1021/jp709592x
25. I.M. El-Naggar, E.A. Mowafy, Y.F. El-Aryan, M.G. Abd El-Wahed, Solid State Ionics **178**, 741 (2007). https://doi.org/10.1016/j.ssi.2007.03.009
26. M.E. Mahmoud, G.M. Nabil, S.M.E. Mahmoudet, J. Environ. Chem. Eng. **3**, 1320 (2015). https://doi.org/10.1016/j.jece.2014.11.027
27. D. Skoda, A. Styskalik, Z. Moravec, P. Bezdicka, J. Pinkas, J. Mater. Sci. **50**, 3371 (2015). https://doi.org/10.1007/s10853-015-8888-1
28. S. Nazer, A.N. Chermahini, B.H. Monjezi, H.A. Dabbagh, J. Taiwan Inst. Chem. Eng. **114**, 168 (2020). https://doi.org/10.1016/j.jtice.2020.09.007
29. B. El-Gammal, S.A. Shady, Colloids. Surf. **287**, 132 (2006). https://doi.org/10.1016/j.colsurfa.2006.02.068
30. J.M. Palomino, D.T. Tran, A.R. Kareh, Ch.A. Miller, J.M.V. Gardner, H. Dong, S.R.J. Oliver, J. Power Sources **278**, 141 (2015). https://doi.org/10.1016/j.jpowsour.2014.12.043
31. Ch. Yue, P.C.M.M. Magusin, B. Mezari, M. Rigutto, E.J.M. Hensen, Microporous Mesoporous Mater. **180**, 48–55 (2013). https://doi.org/10.1016/j.micromeso.2013.06.032
32. T.M.B. Campos, N.C. Ramos, J.D.M. Matos, G.P. Thim, R.O.A. Souza, M.A. Bottino, L.F. Valandro, R.M. Melo, J. Mech. Behav. Biomed. Mater. **109**, 103774 (2020). https://doi.org/10.1016/j.jmbbm.2020.103774.
33. V.V. Baghramyan, A.A. Sargsyan, A.S. Sargsyan, N.B. Knyayan, V.V. Harutyunyan, E.M. Aleksanyan, N.E. Grigoryan, A.H. Badalyan, Arm. J. Phys. **10**(1), 56 (2017)
34. V.I. Yakovlev, V.V. Strelko, M.V. Kravchenko, Sol–gel method of obtaining spherically granular highly porous zirconium silicate. UA Patent 105,999 (2016) **(in Ukrainian)**
35. A. Clearfield, A.I. Bortun, S.A. Khainakov, L.N. Bortun, V.V. Strelko, V.N. Khryaschevskii, Waste Manag. **18**, 203 (1998)
36. I.Z. Zhuravlev, V.A. Kanibolotsky, V.V. Strelko, G.P. Gallios, Sep. Sci. Technol. **39**, 287 (2004). https://doi.org/10.1081/SS-120027559
37. V.V. Strelko, J. Sol-Gel Sci. Technol. **68**, 438 (2013). https://doi.org/10.1007/s10971-013-2990-0
38. F. Mahmood, H. Hu, L. Cao, G. Lu, S. Ni, J. Yuan, Ann. Nucl. Energy **125**, 138 (2019). https://doi.org/10.1016/j.anucene.2018.10.031
39. M. Khalil, Y.F. El-Aryan, I.M. Ali, J. Inorg. Organomet. Polym. **26**, 359 (2016). https://doi.org/10.1007/s10904-015-0318-y
40. A. Patterson, Phys Rev. **56**, 972 (1939)
41. K.Y. Foo, B.H. Hameed, Chem. Eng. J. **156**, 2 (2010). https://doi.org/10.1016/j.cej.2009.09.013
42. A. Kaiser, M. Lobert, R. Telle, J. Eur. Ceram. Soc. **28**, 2199 (2008). https://doi.org/10.1016/j.jeurceramsoc.2007.12.040
43. A.M. Neris, J.M. Ferreira, M.G. Fonseca, I.M. Garcia dos Santos, J. Therm. Anal. Calorim. **143**, 3307 (2021). https://doi.org/10.1007/s10973-020-09286-7
44. I. Romanova, S. Kirillov, J. Therm. Anal. Calorim. **132**, 503 (2018). https://doi.org/10.1007/s10973-017-6880-5
45. S. Tong, Sh. Zhang, H. Yin, J. Wang, M. Chen, J. Anal. Appl. Pyrol. **155**, 105074 (2021). https://doi.org/10.1016/j.jaap.2021.105074
46. V. Raju, S. Jaenicke, G.-K. Chuah, Appl. Catal. B **91**(1–2), 92 (2009). https://doi.org/10.1016/j.apcatb.2009.05.010
47. A.V. Redkina, N.V. Kravchenko, N.D. Konovalova, V.V. Strelko, Vopr. Khimii i Khimicheskoi Tekhnologii **2**, 117 (2021). http://udhtu.edu.ua/public/userfiles/file/VHHT/2021/2/Redkina.pdf